Power management on DC microgrid with new DC coupling based on fuzzy logic

Adhi Kusmantoro[1], Irna Farikhah[2]

[1]Department of Electrical Engineering, Faculty of Engineering and Informatics, Universitas PGRI Semarang, Semarang, Indonesia
[2]Department of Mechanical Engineering, Faculty of Engineering and Informatics, Universitas PGRI Semarang, Semarang, Indonesia

Article Info	ABSTRACT
	In DC microgrids, the utilization of renewable energy results in disruptions. This paper proposes coordinated control of multiple batteries using a fuzzy logic controller (FLC). The goal is to regulate the voltage and power on the DC microgrid. Method used with a modified DC coupling configuration. The proposed new DC coupling topology uses 2 photovoltaic (PV) arrays. Part of the PV array output will be stored in the battery, and part will be provided to the DC bus. Apart from being connected to the DC bus, PV array1 (PV-A1) and PV array2 (PV-A2) are also connected to battery 1 (B1) and battery 2 (B2) via a buck converter. Instead, battery 3 (B3) is connected to the public grid source. The results of the study show that with FLC the voltage deviation and DC bus power are lower when in comparison to the proportional integral (PI) controller. As well, voltage on the DC bus response time with FLC produces a settling time of 0.5 seconds and an overshoot of 0.5%, while the PI controller produces a settling time of 1.15 seconds with an overshoot of 27.6%.

Corresponding Author:

Adhi Kusmantoro
Department of Electrical Engineering, Faculty of Engineering and Informatics, Universitas PGRI Semarang
Semarang, Indonesia
Email: adhikusmantoro@upgris.ac.id

1. INTRODUCTION

In the following few years, newly developed energy has reduced the majority of the world's demand for listicles. Microgrids, which integrate renewable energy sources into their distribution systems, are gaining favor as a potential technology. A combination of load demand and resource integration, such as solar panels, wind turbines, diesel generators, and battery storage systems. In order to deliver electrical energy to the consumer, the microgrid integrates a variety of distributed power, load, energy storage, and control devices. A practical and appropriate method for maximizing the usage of distributed energy is microgrid technology [1]. The scientific community is embracing microgrids as the electricity grid of the future. A small-scale energy network made up of loads and distributed energy resources is what is commonly referred to as a microgrid. However, neither has a well-defined concept nor a well-defined scope. The monitoring units are under additional strain due to the integration of renewable energy resources (RER). The RER depends on intermittent natural events, leading to an unreliable power supply. A demand-supply mismatch could result from network instability brought on by RER power production changes. Researchers proposed many strategies to address these issues [2]. To increase the stability of the DC microgrid, a DC bus voltage regulation can be used. Voltage-mode or current-mode proportional integral (PI) controllers are frequently used to manage voltage on the DC bus. However, the main problem with PI controllers is that it might be challenging for them to successfully satisfy both dynamic response performance and stability requirements and stability criteria because they are frequently at odds with one another [3], [4].

To overcome the limitations of PI control and provide fast dynamic response to load fluctuations while PI controller tuning ensures stability, sensorless load current feed-forward control is provided for DC bus voltage regulation. The proposed control strategy is tested on a cascaded converters system that consists of a single-phase inverter followed by a front-end DC-DC bridge dual active (BDA) converter [5]. Ali et al. [6] proposed A feed-forward compensation system for the BDA converter using lookup tables is needed to get a better transient response. Gurumurthy et al. [7]. The feed-forward equation for the load current is used to increase the DC microgrid's transient response. In his method, PI control is used with feed-forward output on the DAB converter. Esteban et al. [8], for the digital predictive current mode control, a high sampling rate analog-to-digital converter (ADC) is required, which samples the predicted average inductor current rather than the actual average inductor current. A single test of the transformer current is performed at the start of each switching cycle. The succeeding switching cycle's phase shift is calculated using the converter's parameter's nominal values. Rodriguez et al. [9], In order to get an enhanced dynamic performance response in resonant DC-DC converters, a control law based on the Lyapunov technique is developed. The suggested approach has no bandwidth restrictions. Aboushady et al. [10] proposed method, the load current and input/output voltages are sampled. Using this data, the PI controller's output is subjected to the estimated phase-shift. Song et al. [11], a PI based resonant (PIBR) controller should be employed to manage the dc-bus voltage and effectively suppress oscillations with dual-path frequency. Wang et al. [12] proposed a virtual impedance-based control approach. Two poles of the resonant controller are placed there at the same frequency as the double-line frequency to produce a large loop gain at that frequency. However, adding more poles will raise the system order, which can decrease dynamic responsiveness and reduce phase margin at other frequencies. The double-line frequency oscillation is suppressed by increasing the impedance of the inductor current feedback channel by adding a band-pass filter. This paper suggests a technique for a dual voltage control loop DC-DC converter's output impedance. The method used is to adjust the feedback voltage loop so that the DC-DC converter will produce better output impedance characteristics [13], [14].

Conventional DC microgrid control systems often involve a variety of time scales for optimization and real-time control. It is difficult for these control approaches to achieve real-time optimization. Even a small disturbance could cause bus voltages and output currents to diverge from their optimum working levels. Furthermore, the majority of real-time controllers are unable to guarantee the fulfillment of newly defined constraints on specific bus voltages due to the separation between steady-state optimization and real-time control. For a DC microgrid, a distributed optimal control approach is suggested [15]. The objectives are to simultaneously reduce generating costs and regulate individual bus voltage. The system is then dynamically led toward optimal operation by the distributed optimum controller. Simulations using a switch-grade microgrid model validate the effectiveness of the suggested controller. If a communication link is lost or unavailable [16], developed a two window DC bus interacting (DWDI) approach to transmitting data across dispersed energy sources. To show the viability of the suggested DWDI system for DC microgrid controller, a simple master-slave control system without a communication link was built in a small-scale DC microgrid experimental setup. Li et al. [17], by exploiting the modularity feature of the BDA, a more efficient and superior power-sharing technique is developed to maintain bus voltage in microgrid applications. By developing a strong bidirectional power-sharing control method between BDAs from various high-voltage buses and low-voltage buses, voltage stability is improved. An enhanced supervisory controller is created by taking into account the non-linearity and uncertainty that maintain constant DC bus voltage and trustworthy power sharing across DABs under various operating conditions. Regarding power-sharing, regulating the voltage on the DC bus, and power quality, it is discovered that the suggested DAB control offers outstanding performance. Baharizadeh et al. [18], a distributed dynamic event-triggered control mechanism was proposed. While accomplishing current sharing across distributed generation (DG) units, the control strategy proposed can eliminate DC bus voltage variance.

Additionally, the suggested approach only needs the DC bus voltage from the physical network and doesn't need any other global information. Additionally, only events that trigger data from nearby DGs are included, which significantly lessens the communication load on the DC microgrid communication network. Xing et al. [19] proposed a switching at zero voltage (SZV) method for a DC-DC converter (DDC) with a large voltage gain and which is used for energy storage on a DC bus microgrid. The current and voltage multiplier are located on the low voltage sides (LVS) and the high voltage sides (HVS), respectively. An 800-W prototype with 48–60 V input and 240 V output is constructed with a switching frequency of 30 kHz to test the performance of the converter and the associated control technique. The agreement between the outcomes of the trial and the analysis further supports the advantages. Zeng et al. [20] proposes a transient modeling approach for a voltage source converter-based DC microgrid (VSCD). Analyzed are the transient properties of the VSCD in the active power control and Control methods for DC bus voltage. After that, a flawed DC microgrid model is created using VSC and DC line models. Incorrect DC microgrid analysis can be successfully employed in the transient modeling approach. The approach suggested in this article can increase the precision of DC microgrid analysis on faults on fault and ensure computation efficiency. In islanded DC

microgrids, this study suggests a distributed secondary control mechanism for exact power distribution and voltage restoration [21]. In order to return the DC bus voltage to its nominal value while maintaining power-sharing precision, the secondary control layer suggests a distributed control strategy. Using the limited understanding of the DC bus voltage and the secondary control inputs of their neighboring controllers, a distributed secondary control input can be built and then delivered to the related primary controller. In contrast to the majority of previous techniques, just DC bus voltage feedback is needed. A distributed DC MG cluster can be created by connecting several nearby distributed dc microgrids (MGs). Isolated bidirectional DC-DC converters (IBDCs) can work as active, coupled devices that enable variable power control and electrical isolation among the DC MGs. A special coordinated power control for such a cluster is offered in the paper [22]. The DC MGs adopt the traditional droop control while the IBDCs have unified management. The droop control method is one of the most used methods for managing the DC microgrid.

To get around the system's non-linearity, this study [23] offers an adaptive-droop technique for dc microgrids. To remove the current sharing error of each unit in the microgrid, the droop- resistance is modified using an adaptive PI (API) controller. The current and voltage at the microgrid's DC bus must be transmitted across minimum bandwidth communication channels to individual units under the proposed approach. Mokhtar *et al.* [24] used a generalized reduced-order modeling approach to demonstrate the dynamic stability of DC voltage management utilizing these 2 modes. An RLC parallel circuit models each DC voltage drop control unit with 2 modes. The method ignores rapid flow changes and is used for modeling and modular expansion. Finally, several recent studies of DC bus voltage regulation in a radial configuration [25]–[29] using a series voltage controller (SVC). This method uses a BAD and a full bridge (FB) DC-DC converter. To counteract resistive drop across the network, it adds dynamic voltage to the DC grid in series. The voltage level at the various grid nodes, as a result, becomes resistant to changes in load and keeps the predetermined limit. The findings demonstrate the usefulness of such a voltage regulator (VR) for radial for DC microgrids, particularly in severe load conditions.

All studies have not used battery management strategies properly when renewable energy sources are disconnected and when the DC microgrid operates on an island. In this study, the voltage to the DC bus is regulated utilizing a multiple source control method with a fuzzy logic controller (FLC). DC microgrid uses a modified DC coupling topology. With the new design and multi-source DC bus, voltage stability will be achieved. The photovoltaic (PV) is connected to the battery via a buck converter in the older DC coupling configuration. When the weather is sunny, the PV output will be stored in the battery. The battery is the only source of power for the DC bus. Maximum power point tracking (MPPT) will allow the PV to operate at its full output while saving energy to the battery in island mode. Therefore, several recent studies have discussed battery control for supply to the DC bus [30]–[33]. The proposed new DC coupling configuration uses two PV arrays. Part of the output of the PV array will be stored in the battery, and some will be supplied to the DC bus. PV array1 (PV-A1) and PV array2 (PV-A2), besides being connected to the DC bus, are also connected to battery 1 (B1) and battery 2 (B2) via a buck converter. In this new DC coupling configuration, battery 3 (B3) is charged with a rectifier source from the utility grid. The battery capacity is calculated based on the magnitude of the DC load. Using multi-source, the DC bus voltage stability will be fulfilled, compared to the old DC coupling configuration method. Based on previous studies, PI controls are widely used in renewable energy settings and provide energy flow results with a less rapid response. In addition, FLC have also been widely used to regulate energy flow and provide a faster response and load power stability for the purpose when compared to PI controls. Therefore, we suggest using a FLC to adjust the battery's energy flow to the load or DC bus. In the end, FLC will adapt the output from each DC source to the microgrid DC bus. The controller will stabilize voltage on the DC bus at 48 V and supply the DC bus from each source alternately. The proposed microgrid DC works in grid-connected mode.

After explaining the previous research in the introduction, we organize this article in section 2: Method. This section contains modeling of DC microgrid, proposed method, explanation of the design of the FLC for controlling the flow of battery power. Section 3: Discusses the results obtained for the new DC-coupling system configuration. In section 4: Conclusions on the results of research that has been done.

2.   METHOD

In a DC microgrid, the conventional droop control method entails linearly lowering the voltage reference as the output current increases. The decrease in the current sharing accuracy is the droop control method's limitation. The increased voltage droop across the line resistances prevents the output voltage from being precisely the same. Consequently, the load current sharing's accuracy is decreased, causing the voltage to deviate owing to drooping. Dividing the microgrid DC load current can be implemented with an I-V droop controller, which determines the adaptive voltage. From several studies when the line resistance using droop control will cause different load currents [34]–[37].

2.1. Modeling of DC microgrid

Figure 1 illustrates a DC microgrid, utilizing an analogous circuit model. The DC microgrid has two voltage sources which are part of the converter. DC current will flow from each source to the load through the long line.
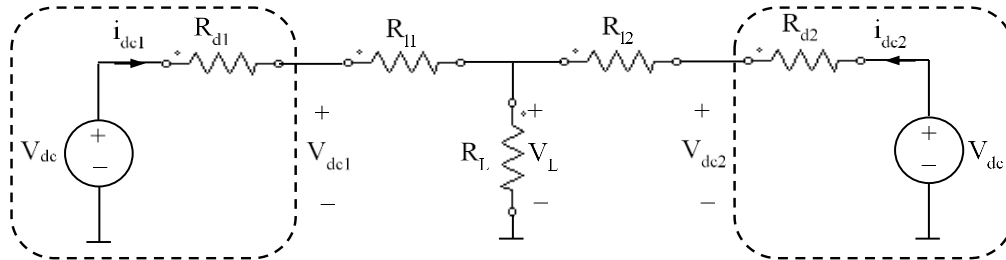
Figure 1. DC microgrid modeling with control of droop

The equation can be used to describe how droop control is used in a DC microgrid as shown in (1):

$$v_{dcj} = v_{dc} - i_{dcj}R_{dj} \tag{1}$$

where v_{dcj}, v_{dc}, i_{dcj}, R_{dj} are DC voltage node, source of DC voltage, source of DC current, and virtual resistance of each DC source (j = 1, 2, …). As illustrated in Figure 1, the output voltage of each source is similar to V_{dc}, and the virtual resistance expressed in (1) is equal to the output resistance. While the load voltage equation can be defined as shown in (2) and (3).

$$V_L = v_{dc} - i_{dc1}R_{d1} - i_{dc1}R_{l1} \tag{2}$$

$$V_L = v_{dc} - i_{dc2}R_{d2} - i_{dc2}R_{l2} \tag{3}$$

The above equation shows that in a DC microgrid with droop control, DC microgrid virtual resistance is inversely proportional to each current source. We can assume that the DC microgrid is a small-scale network and the resistance R_l is minimal, so that it is possible to select the virtual resistance R_{dj} as significant. However, the presumption above works for a huge R_{dj}. Several studies state precise current sharing can not be guaranteed for R_{dj}. Large virtual resistance, but cannot guarantee voltage regulation [38]–[41].

Figure 2 displays the voltage variation with various virtual resistances. The voltage deviation is zero when the sources are operating in an open circuit state (with no source currents), as shown in Figure 3. Voltage deviation occurs when the current from the sources is not zero; the magnitude of this deviation changes with the load. The droop coefficient R_{dj} and should be limited to keep the output voltage variation under control. The following equation expresses the difference in voltage at the node as shown in (4).

$$\Delta v_{dc} = v_{dc} - v_{dcj} = i_{dcj}R_{dj} \tag{4}$$
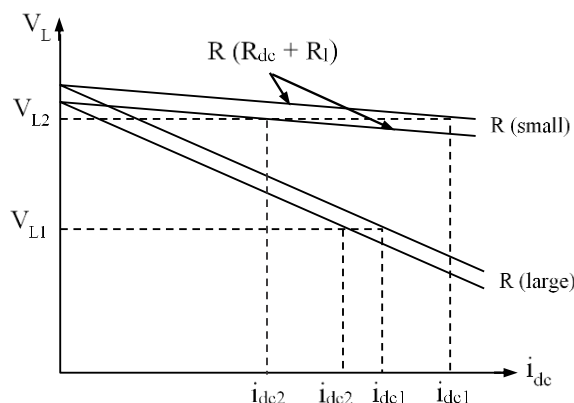
Figure 2. Droop curve with different virtual resistance
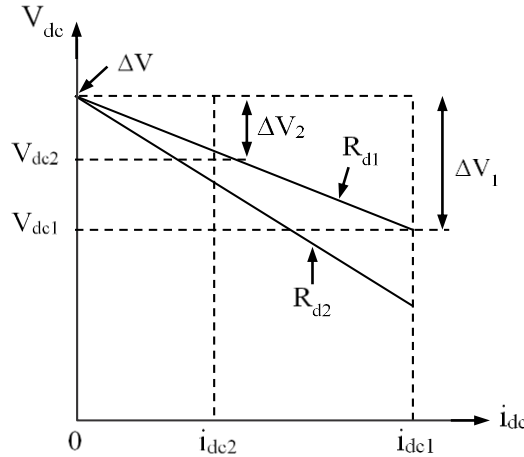
Figure 3. The voltage's deviation with the change in the droop coefficient

2.2. Proposed method

A modified DC-coupling configuration is proposed on a multiple source DC microgrid. In this DC microgrid system, a battery storage unit is used, both from the PV source side and the source side of the utility grid. The PV array output is used for the PV-side load and battery charging. In this second model, the utility grid's voltage is transformed into DC voltage using a rectifier.

The resulting DC voltage is used for the utility grid-side battery charging process. When the PV output voltage is cut off, the PV-side battery supplies the load, the utility grid-side battery will operate when the PV-side battery can no longer supply the load. The purpose of this DC microgrid configuration is always to meet load requirements. The benefit of utilizing a battery storage system on the PV-side and the utility grid-side is that if one battery is insufficient to supply voltage to the DC bus, two batteries will quickly supply voltage to the DC bus. Figure 4 shows a modified DC-coupling structure. This model has an additional rectifier circuit to charge the battery. The PV module used has voltage is an open circuit $V_{oc} = 21.6$ V, a series's number of cells $N_s = 36$, the number of parallel cells $N_p = 1$, the maximum voltage $V_{mp} = 18$ V, power $P_{mp} = 60$ W. While the battery used is a Lithium-Ion battery with a nominal voltage of 12 V, a rated capacity of 65 Ah, and an initial the state of charge (SOC) of 50%.
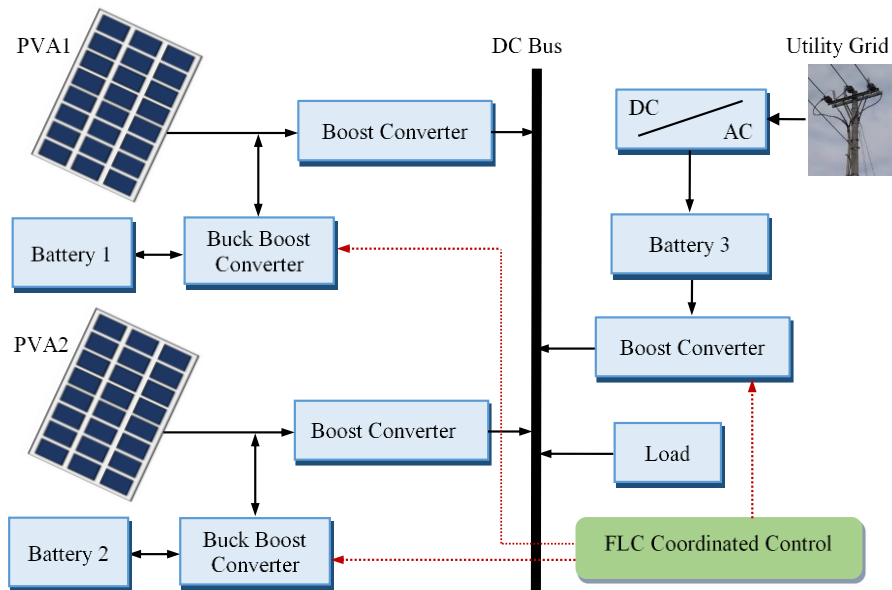
Figure 4. New DC-coupling configuration for the DC microgrid

Figure 5 depicts the planned DC microgrid configuration modelled. If V_g is the nominal voltage of each source of the distributed generator, V_{dc} is the voltage on the DC bus, i_l is the output current, and R_d is the current-voltage droop, then the output voltage of the distributed generator supplied to the DC bus is as (5).

$$v_{dc} = v_g - i_{dc}R_d \qquad (5)$$
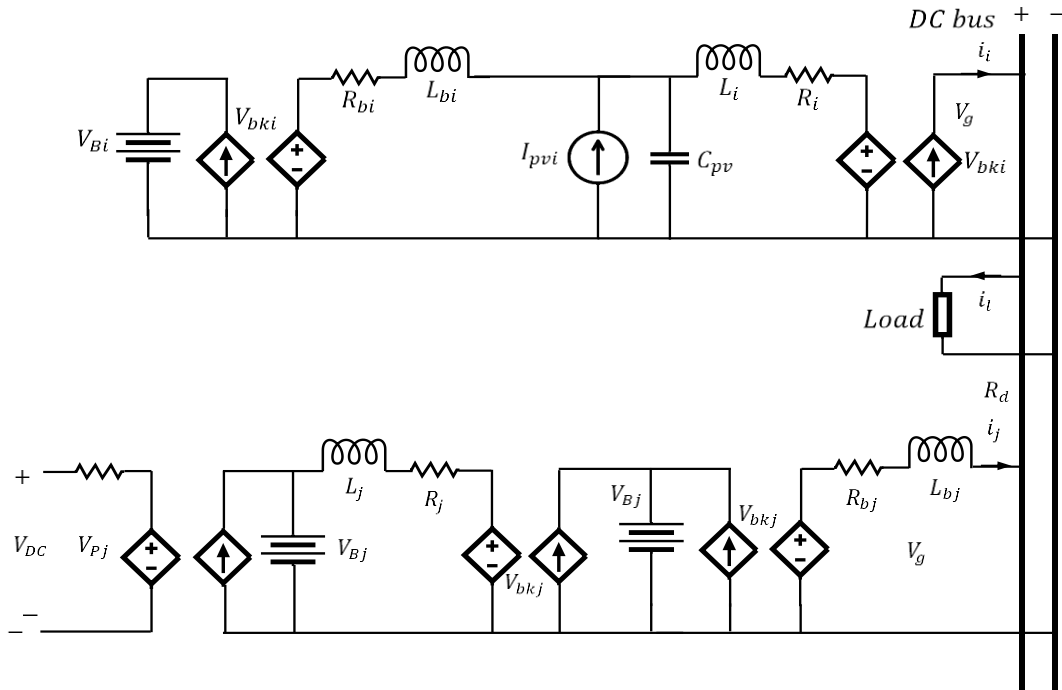
Figure 5. Modeling the new DC microgrid configuration

2.3. Design of FLC

Several previous studies regarding the design of FLC on DC microgrids are as follows. Qu *et al.* [42] proposes FLC to escalate load power-sharing and DC bus voltage changes in a balanced way when renewable energy sources fluctuate. This study uses two FLCs. FLC1 functions for power distribution, and FLC2 functions for voltage regulation. The test results show the advantages of FLC compared to conventional controls. Peña-Aguirre *et al.* [43] proposed a microgrid power management system using FLC to maintain a power balance in the microgrid. FLC has two inputs: the SOC battery and power microgrid (PMG). The FLC can regulate battery usage and power flow from various sources and loads. In addition, FLC can reduce battery usage. In several studies [44], [45] the authors used a solid-state transformer for the converter in a microgrid system. Control coordination in energy management settings using FLC. FLC can regulate the flow of energy between solid-state transformers on the converter. The proposed method is to reduce the voltage changes on the DC bus. The study offers a power flow arrangement of a hybrid storage system from batteries and ultra-capacitors using FLC. The FLC determines the reference current for the input of the storage unit converter so changes voltage in the DC bus can be controlled. The proposed method is superior when compared to PI/ proportional integral derivative (PID) controller. Also, in the study FLC was designed to manage a DC microgrid energy management system. The system uses eight modes to minimize energy use costs. FLC is designed with two inputs: grid price and the optimization factor. FLC can improve microgrid performance in energy management.

The voltage differences in each converter connected to PV in a DC microgrid will cause a difference in the current of each converter to the load. In addition, several PV sources have different characteristics, and when there is a change in the voltage at R_l, it will cause problems with the DC bus voltage. Therefore, a FLC is proposed as part of a battery management technique. The setting of each battery is done by limiting the use of SOC to the minimum and maximum limits when charging from PV. With the FLC strategy, there is a setting for the use benefit of each battery. The following equation expresses the change in SOC.

Figure 6 shows the FLC design used in this study. FLC is designed to use 2 inputs and 1 output. The first input is the second is the DC voltage difference (ΔV) in Figure 6(a), and the SOC difference in Figure 6(b).

While the output is a change in the voltage on the DC bus (ΔVo) in Figure 6(c). The difference in DC voltage (ΔV) is the difference between the DC bus reference voltage and the voltage of each battery, which is expressed by the (6) and (7).

$$\Delta V = V_{ref} - \Delta V_b \qquad\qquad (6)$$

$$\Delta V_{min} \leq \Delta V \leq \Delta V_{max} \qquad\qquad (7)$$

The control technique for supplying battery power and voltage to the DC bus is shown in Figure 7. Each battery is also set to the lowest and highest SOC limits so that the battery does not run out when operating and discharging. Figure 7 shows that FLC has two inputs.

(a)

(b)

(c)
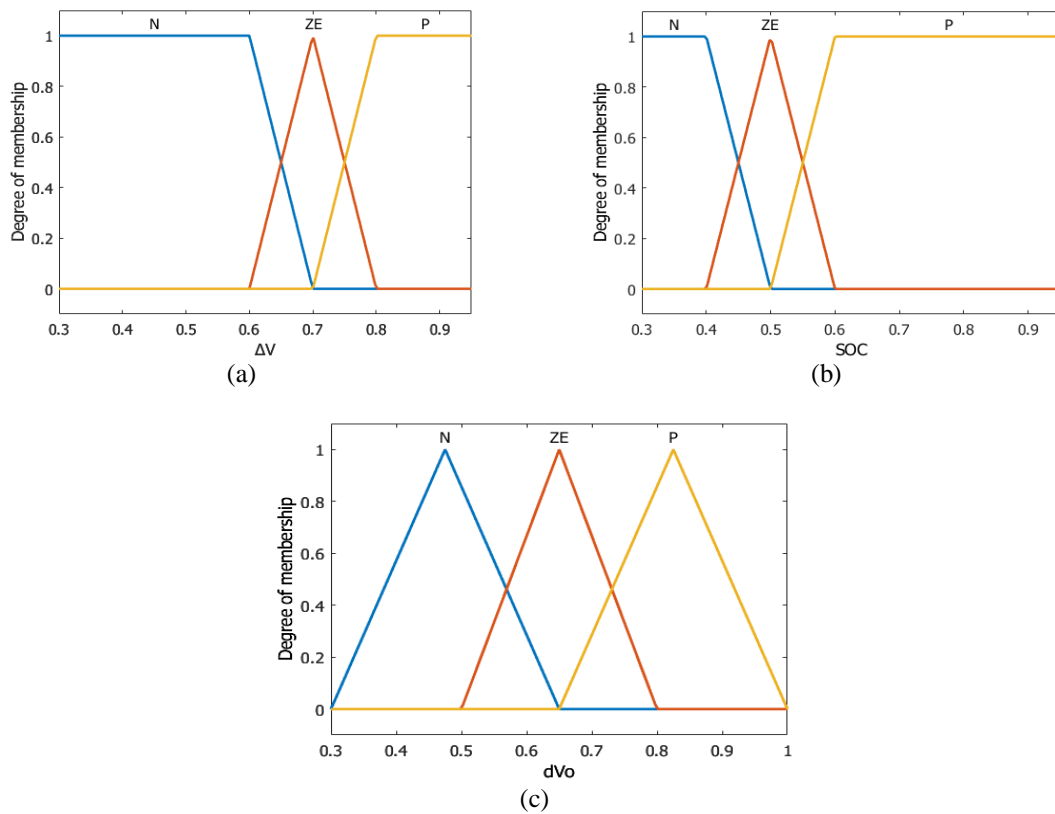
Figure 6. Battery control strategy membership function: (a) ΔV membership function, (b) SOC membership function, and (c) dVo membership function
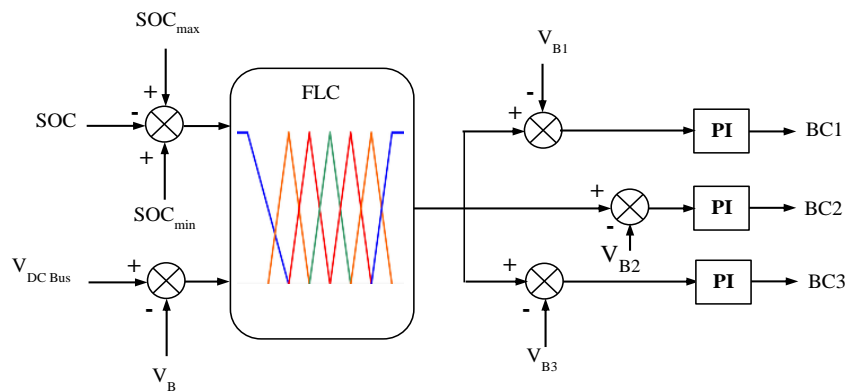
Figure 7. FLC control strategy on multiple battery

The difference between the SOC and the difference between voltage on the DC bus and the battery voltage. When a battery power supply is needed, or there is a difference between the standard voltage and battery voltage 1 (B1), the first PI control will adjust the boost converter 1 (BC1) output. When SOC B1 is minimum, and there is a voltage difference with B2, the second PI control will change the output of boost converter 2 (BC2). And so on, when the SOC B2 is minimum, the third PI controller will change the output of boost converter 3 (BC3).

3. RESULTS AND DISCUSSION

A DC microgrid study with a new DC coupling configuration conducted in Semarang, Indonesia. The study will be conducted in 2022, with an average solar radiation intensity of 4.8 kWh/m^2. The variables utilized in the DC microgrid study are displayed in Table 1. In this study, using MATLAB software. In this study, the excess output power of each PV array is stored in the battery, while the 3-charging battery uses a utility grid source.

Table 1. Study parameter on DC microgrid

Parameter	Value
Maximum power output of PV-A1	80 kWp
Maximum power output of PV-A2	80 kWP
Rated DC bus voltage	500 V
Battery 1 (B1)	500 V, 75 Ah
Battery 2 (B2)	500 V, 75 Ah
Battery 3 (B3)	500 V, 60 Ah
Maximum output power DC load	75 kW

3.1. Case 1 (PV supply to load)

Figure 8 displays the PV array's output for the DC microgrid. The power produced by the PV array is larger than the DC load utilised. However, not all the PV array output power is given to the load but is stored in the battery. PV-A1 and PV-A2 are located at different locations with varying solar radiation intensities. PV-A1 produces 80 kW of output power, while PV-A2 also produces 80 kW of output power. At 0.5 seconds to 2.3 seconds, there is a difference in output power between PV-A1 and PV-A2 due to differences in the intensity of solar radiation. However, at 2.5 seconds, the peak output power of PV-A1 and PV-A2 is 80 kW. The difference in output power of PV-A1 and PV-A2 also occurs from 0.27 seconds to 4.5 seconds. In addition, in Figure 8, it can be seen that the peak load of 75 kW occurs at 1.7 seconds and the lowest load of 30 kW occurs at 1.3 seconds.
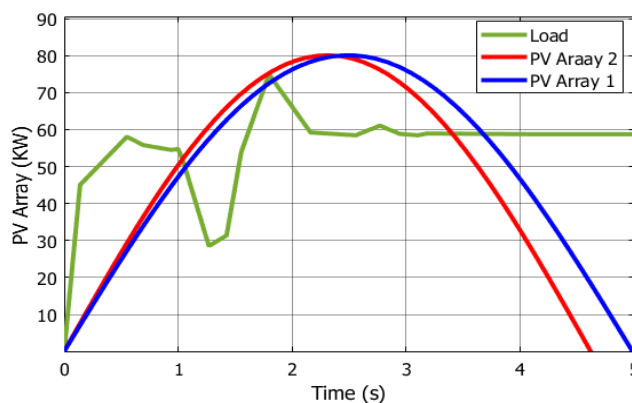
Figure 8. Output power of a PV array and DC load

The DC bus is supplied from the PV array output for load requirements in the first case. However, the increase in voltage until it reaches the nominal DC bus voltage of 500 V is affected by the PV array output, Figure 9. From 0 seconds to 0.5 seconds, there is a voltage deviation of 6 V, while from 0.5 seconds to 1 second, there is a voltage deviation of 3 V. The DC voltage stability is achieved at 1 second to 4 seconds. The DC bus voltage deviation also occurs from 4 seconds to 5 seconds, the intensity of solar radiation influences this.

Due to changes in load when using a PV array source, the load current also changes according to changes in load. Figure 10 shows the difference in load current when using a PV array source. Figure 10, shows that the peak current of 150 A occurred at 1.7 seconds and the lowest current of 95 A occurred at 1.3 seconds. An ever-increasing load will result in a change in current from the output of the PV array. This shows that in this study the PV array used is capable of supplying power at peak loads.
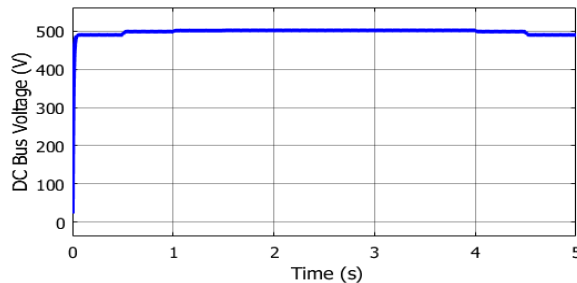
Figure 9. DC bus voltage with PV array   Figure 10. Load current
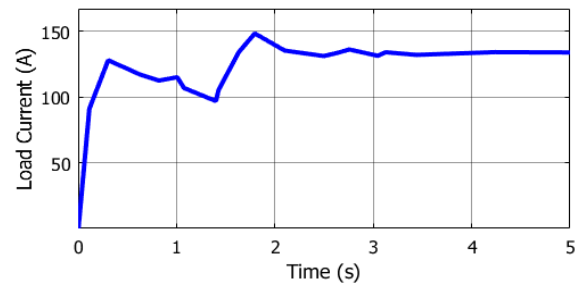
3.2. Case 2 (Battery suplly to load)

The battery in the second case is used to fulfill the demand when the PV array output is disconnected or intermittent. FLC is used in the distribution of battery power, whose performance is compared to the PI control and the PID control strategy. The battery output power setting is shown in Figure 11 due to the DC load demand.

The battery on the PV side is storage battery 1 (B1) and storage battery 2 (B2), while the battery on the grid side is battery 3 (B3). Setting the output power B1 to B3 using the FLC control strategy. Figure 11 shows the setting of the battery output power to the load. At 0 seconds to 2 seconds using B1. When the output of B1 drops, then B2 at 2 seconds to 4.5 seconds supplies power to the load through the DC bus. When the output of B2 drops then B3 at 4.5 seconds to 5 seconds supplies power to the load. Figure 12 shows the load current between the battery source and the PV array source has been disconnected. The load current looks stable at 4.5 seconds with the FLC strategy. It shows the maximum battery output power when using FLC. In addition, at 2 seconds, a high current transient occurs when using the PI and PID controls, with a peak of 70 A.
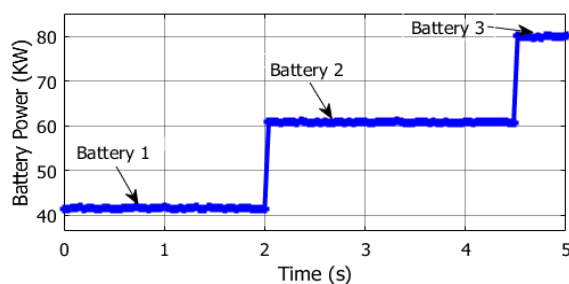
Figure 11. Battery output power   Figure 12. Load current with a battery source
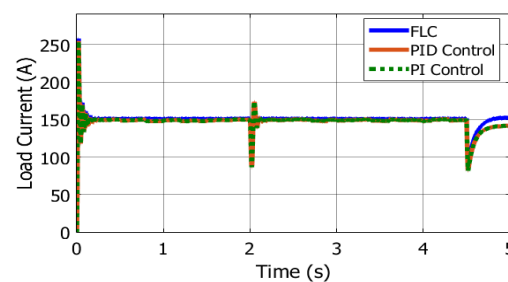
Figure 13 shows the response time of the DC bus voltage with sources B1 to B3 with PI, PID, and FLC controllers. Based on the response time in Figure 13, the battery management strategy with FLC shows better battery performance compared to PI and PID controllers. The battery source on the microgrid is used to supply the load when the PV array output is disconnected. The battery management strategy is carried out to address the ever-changing and increasing load requirements.

The PI control produces a settling time of 1.15 seconds with a 27.6% overshoot. At the same time, the settling time for the PID controller is 0.86 seconds and a 17.4% overshoot. FLC produces a settling time of 0.5 seconds and 0.5% overshoot. FLC response time parameters are faster than PI and PID controls, as shown in Table 2. Table 3 compares the effectiveness of power and voltage distribution on the DC bus for the DC-microgrid coordinated control using FLC with PI and PID controls. FLC coordinated control can supply maximum power and current to the load compared to PI and PID controls.
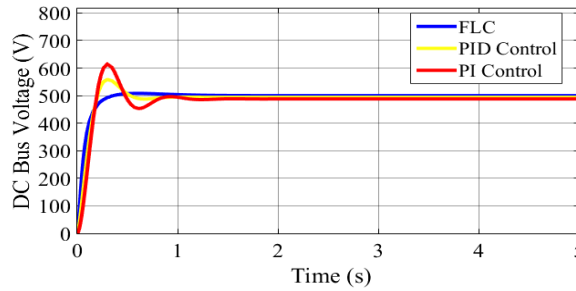
Figure 13. DC bus voltage response time

Table 2. Response time for DC bus voltage

Controller type	Rise time/tr (s)	Settling time/ts (s)	Overshoot/Mp (%)
PI controller	0.082	1.15	27.60
PID controller	0.043	0.86	17.40
FLC	0.016	0.50	0.50

Table 3. Coordinated control on DC microgrid

Parameter	PI controller	PID controller	FLC
DG unit power of PV	159 kW	160 kW	160 kW
Battery power	152 kW	155 kW	158 kW
DC bus voltage	487 V	494 V	500 V
Deviasi bus voltage	13 V	6 V	0 V
Maximum load current	2.6%	1.2%	0%

4.   CONCLUSION

Coordinated control strategy on multi-battery is used to improve voltage and power stability in DC microgrid development with new DC coupling configuration. In the battery management strategy, a FLC is used by alternating battery output. This control method can produce stable voltage and on the DC bus's power, when the PV array output is disconnected or when there is no solar radiation intensity. According to the study's findings, FLC has a lower DC bus voltage transient than PI control. As well, the deviation of the battery output voltage with FLC is also minimum when compared to the PI controller. Battery output power with FLC is also maximum, with low current transients. By using FLC, there is an increase in the DC bus voltage's stability.

ACKNOWLEDGEMENTS

REFERENCES

[1]   X. Liu, T. Zhao, H. Deng, P. Wang, J. Liu, and F. Blaabjerg, "Microgrid energy management with energy storage systems: A review," *CSEE Journal of Power and Energy Systems*, vol. 9, no. 2, pp. 483–504, 2023, doi: 10.17775/CSEEJPES.2022.04290.
[2]   B. Zhao *et al.*, "Energy management of multiple microgrids based on a system of systems architecture," *IEEE Transactions on Power Systems*, vol. 33, no. 6, pp. 6410–6421, 2018, doi: 10.1109/TPWRS.2018.2840055.
[3]   H. Novak, V. Lesic, and M. Vasak, "Hierarchical model predictive control for coordinated electric railway traction system energy management," *IEEE Transactions on Intelligent Transportation Systems*, vol. 20, no. 7, pp. 2715–2727, 2019, doi: 10.1109/TITS.2018.2882087.
[4]   M. S. Agamy *et al.*, "A high power medium voltage resonant dual active bridge for MVDC ship power networks," *IEEE Journal of Emerging and Selected Topics in Power Electronics*, vol. 5, no. 1, pp. 88–99, 2017, doi: 10.1109/JESTPE.2016.2636365.
[5]   M. T. Iqbal and A. I. Maswood, "An explicit discrete-time large- and small-signal modeling of the dual active bridge DC–DC converter based on the time scale methodology," *IEEE Journal of Emerging and Selected Topics in Industrial Electronics*, vol. 2, no. 4, pp. 545–555, 2021, doi: 10.1109/jestie.2021.3087942.
[6]   M. Ali, M. Yaqoob, L. Cao, and K. H. Loo, "Enhancement of DC-bus voltage regulation in cascaded converter system by a new sensorless load current feedforward control scheme," *IET Power Electronics*, vol. 14, no. 8, pp. 1457–1467, 2021, doi: 10.1049/pel2.12123.
[7]   S. K. Gurumurthy, M. Mirz, B. S. Amevor, F. Ponci, and A. Monti, "Hybrid dynamic phasor modeling approaches for accurate closed-loop simulation of power converters," *IEEE Access*, vol. 10, no. September, pp. 101643–101655, 2022, doi: 10.1109/ACCESS.2022.3208963.
[8]   F. D. Esteban, F. M. Serra, and C. H. D. Angelo, "Control of a DC-DC dual active bridge converter in DC microgrids applications," *IEEE Latin America Transactions*, vol. 19, no. 8, pp. 1261–1269, 2021, doi: 10.1109/TLA.2021.9475856.

[9]   J. R. Rodriguez-Rodriguez, N. M. Salgado-Herrera, J. Torres-Jimenez, N. Gonzalez-Cabrera, D. Granados-Lieberman, and M. Valtierra-Rodriguez, "Small-signal model for dual-active-bridge converter considering total elimination of reactive current," *Journal of Modern Power Systems and Clean Energy*, vol. 9, no. 2, pp. 450–458, 2021, doi: 10.35833/MPCE.2018.000911.

[10] A. A. Aboushady, K. H. Ahmed, S. J. Finney, and B. W. Williams, "Lyapunov-based high-performance controller for modular resonant DC/DC converters for medium-voltage DC grids," *IET Power Electronics*, vol. 10, no. 15, pp. 2055–2064, 2017, doi: 10.1049/iet-pel.2017.0180.

[11] W. Song, N. Hou, and M. Wu, "Virtual direct power control scheme of dual active bridge DC-DC converters for fast dynamic response," *IEEE Transactions on Power Electronics*, vol. 33, no. 2, pp. 1750–1759, 2018, doi: 10.1109/TPEL.2017.2682982.

[12] D. Wang, B. Nahid-Mobarakeh, and A. Emadi, "Second harmonic current reduction for a battery-driven grid interface with three-phase dual active bridge DC-DC converter," *IEEE Transactions on Industrial Electronics*, vol. 66, no. 11, pp. 9056–9064, 2019, doi: 10.1109/TIE.2019.2899563.

[13] W. Wang *et al.*, "Power decoupling control for single-phase grid-tied PEMFC systems with virtual-vector-based MPC," *IEEE Access*, vol. 9, pp. 55132–55143, 2021, doi: 10.1109/ACCESS.2021.3071776.

[14] L. Zhang *et al.*, "Modeling, control, and protection of modular multilevel converter-based multi-terminal HVDC systems: A review," *CSEE Journal of Power and Energy Systems*, vol. 3, no. 4, pp. 340–352, 2017, doi: 10.17775/cseejpes.2017.00440.

[15] L. Cao, K. H. Loo, and Y. M. Lai, "Output-impedance shaping of bidirectional DAB DC-DC converter using double-proportional-integral feedback for near-ripple-free DC bus voltage regulation in renewable energy systems," *IEEE Transactions on Power Electronics*, vol. 31, no. 3, pp. 2187–2199, 2016, doi: 10.1109/TPEL.2015.2433535.

[16] J. Peng, B. Fan, and W. Liu, "Voltage-based distributed optimal control for generation cost minimization and bounded bus voltage regulation in DC microgrids," *IEEE Transactions on Smart Grid*, vol. 12, no. 1, pp. 106–116, 2021, doi: 10.1109/TSG.2020.3013303.

[17] F. Li, Z. Lin, Z. Qian, J. Wu, and W. Jiang, "A dual-window DC bus interacting method for DC microgrids hierarchical control scheme," *IEEE Transactions on Sustainable Energy*, vol. 11, no. 2, pp. 652–661, 2020, doi: 10.1109/TSTE.2019.2900617.

[18] M. Baharizadeh, M. S. Golsorkhi, M. Shahparasti, and M. Savaghebi, "A two-layer control scheme based on P-V droop characteristic for accurate power sharing and voltage regulation in DC microgrids," *IEEE Transactions on Smart Grid*, vol. 12, no. 4, pp. 2776–2787, 2021, doi: 10.1109/TSG.2021.3060074.

[19] L. Xing, F. Guo, X. Liu, C. Wen, Y. Mishra, and Y. C. Tian, "Voltage restoration and adjustable current sharing for DC microgrid with time delay via distributed secondary control," *IEEE Transactions on Sustainable Energy*, vol. 12, no. 2, pp. 1068–1077, 2021, doi: 10.1109/TSTE.2020.3032605.

[20] J. Zeng, Z. Yan, J. Liu, and Z. Huang, "A high voltage-gain bidirectional DC-DC converter with full-range ZVS using decoupling control strategy," *IEEE Journal of Emerging and Selected Topics in Power Electronics*, vol. 8, no. 3, pp. 2775–2784, 2020, doi: 10.1109/JESTPE.2019.2911331.

[21] H. Nian and L. Kong, "Transient modeling and analysis of VSC based DC microgrid during short circuit fault," *IEEE Access*, vol. 7, pp. 170604–170614, 2019, doi: 10.1109/ACCESS.2019.2955379.

[22] F. Guo, Q. Xu, C. Wen, L. Wang, and P. Wang, "Distributed secondary control for power allocation and voltage restoration in islanded DC microgrids," *IEEE Transactions on Sustainable Energy*, vol. 9, no. 4, pp. 1857–1869, 2018, doi: 10.1109/TSTE.2018.2816944.

[23] X. Li *et al.*, "Flexible interlinking and coordinated power control of multiple DC microgrids clusters," *IEEE Transactions on Sustainable Energy*, vol. 9, no. 2, pp. 904–915, 2018, doi: 10.1109/TSTE.2017.2765681.

[24] M. Mokhtar, M. I. Marei, and A. A. El-Sattar, "An adaptive droop control scheme for DC microgrids integrating sliding mode voltage and current controlled boost converters," *IEEE Transactions on Smart Grid*, vol. 10, no. 2, pp. 1685–1693, 2019, doi: 10.1109/TSG.2017.2776281.

[25] P. Li *et al.*, "Reduced-order modeling and comparative dynamic analysis of DC voltage control in DC microgrids under different droop methods," *IEEE Transactions on Energy Conversion*, vol. 36, no. 4, pp. 3317–3333, 2021, doi: 10.1109/TEC.2021.3076438.

[26] U. Vuyyuru, S. Maiti, C. Chakraborty, and B. C. Pal, "A series voltage regulator for the radial DC microgrid," IEEE Transactions on Sustainable Energy, vol. 10, no. 1, pp. 127–136, 2019, doi: 10.1109/TSTE.2018.2828164.

[27] N. Bayati, H. R. Baghaee, A. Hajizadeh, and M. Soltani, "Localized protection of radial DC microgrids with high penetration of constant power loads," IEEE Systems Journal, pp. 1–12, 2020, doi: 10.1109/JSYST.2020.2998059.

[28] D. Miller, G. Mirzaeva, C. D. Townsend, and G. C. Goodwin, "Decentralised droopless control of islanded radial AC microgrids without explicit communication," *IEEE Open Journal of Industry Applications*, vol. 3, no. April, pp. 104–113, 2022, doi: 10.1109/ojia.2022.3177857.

[29] L. F. Grisales-Noreña, O. D. Montoya, and C. A. Ramos-Paja, "An energy management system for optimal operation of BSS in DC distributed generation environments based on a parallel PSO algorithm," J. Energy Storage, vol. 29, pp. 101488, 2020, doi: 10.1016/j.est.2020.101488.

[30] O. D. Montoya, W. Gil-Gonzalez, and A. Garces, "Optimal power flow on DC microgrids: A quadratic convex approximation," *IEEE Transactions on Circuits and Systems II: Express Briefs*, vol. 66, no. 6, pp. 1018–1022, 2019, doi: 10.1109/TCSII.2018.2871432.

[31] N. Kumar, I. Hussain, B. Singh, and B. K. Panigrahi, "Single sensor-based MPPT of partially shaded PV system for battery charging by using cauchy and gaussian sine cosine optimization," *IEEE Transactions on Energy Conversion*, vol. 32, no. 3, pp. 983–992, 2017, doi: 10.1109/TEC.2017.2669518.

[32] Q. Yan, S. Member, B. Zhang, S. Member, and M. Kezunovic, "Optimized operational cost reduction for an ev charging station integrated with battery energy storage and PV generation," *IEEE Transactions on Smart Grid,* vol. 10, no. 2, pp. 2096–2106, 2019, doi: 10.1109/TSG.2017.2788440.

[33] C. Tang, P. Chen, and J. Jheng, "Bidirectional Power flow control and hybrid charging strategies for three-phase PV power and energy storage systems," *IEEE Transactions on Smart Grid,* vol. 36, no. 11, pp. 12710-12720, 2021, doi: 10.1109/TPEL.2021.3083366.

[34] X. Li and S. Wang, "Energy management and operational control methods for grid battery energy storage systems," *CSEE Journal of Power and Energy Systems*, vol. 7, no. 5, pp. 1026–1040, 2021, doi: 10.17775/CSEEJPES.2019.00160.

[35] Y. Han, X. Ning, P. Yang, and L. Xu, "Review of power sharing, voltage restoration and stabilization techniques in hierarchical controlled DC microgrids," *IEEE Access*, vol. 7, pp. 149202–149223, 2019, doi: 10.1109/ACCESS.2019.2946706.

[36] A. H. Yazdavar, M. A. Azzouz, and E. F. El-Saadany, "A novel decentralized control scheme for enhanced nonlinear load sharing and power quality in islanded microgrids," *IEEE Transactions on Smart Grid*, vol. 10, no. 1, pp. 29–39, 2019, doi: 10.1109/TSG.2017.2731217.

[37]   Y. Qi, P. Lin, Y. Wang, and Y. Tang, "Two-dimensional impedance-shaping control with enhanced harmonic power sharing for inverter-based microgrids," *IEEE Transactions on Power Electronics*, vol. 34, no. 11, pp. 11407–11418, 2019, doi: 10.1109/TPEL.2019.2898670.

[38]   Z. Li, Z. Cheng, J. Si, and S. Li, "Distributed event-triggered secondary control for average bus voltage regulation and proportional load sharing of DC microgrid," *Journal of Modern Power Systems and Clean Energy*, vol. 10, no. 3, pp. 678–688, 2022, doi: 10.35833/MPCE.2020.000780.

[39]   S. Chaturvedi and D. Fulwani, "Adaptive voltage tuning based load sharing in DC microgrid," *IEEE Transactions on Industry Applications*, vol. 57, no. 1, pp. 977–986, 2021, doi: 10.1109/TIA.2020.3034068.

[40]   M. Rashad, U. Raoof, M. Ashraf, and B. A. Ahmed, "Proportional load sharing and stability of DC microgrid with distributed architecture using SM controller," *Mathematical Problems in Engineering*, vol. 2018, 2018, doi: 10.1155/2018/2717129.

[41]   D. H. Dam and H. H. Lee, "A power distributed control method for proportional load power sharing and bus voltage restoration in a DC microgrid," *IEEE Transactions on Industry Applications*, vol. 54, no. 4, pp. 3616–3625, 2018, doi: 10.1109/TIA.2018.2815661.

[42]   Z. Qu, Z. Shi, Y. Wang, A. Abu-Siada, Z. Chong, and H. Dong, "Energy management strategy of AC/DC hybrid microgrid based on solid-state transformer," *IEEE Access*, vol. 10, pp. 20633–20642, 2022, doi: 10.1109/ACCESS.2022.3149522.

[43]   J. C. Pena-Aguirre, A. I. Barranco-Gutierrez, J. A. Padilla-Medina, A. Espinosa-Calderon, and F. J. Perez-Pinal, "Fuzzy logic power management strategy for a residential DC-microgrid," *IEEE Access*, vol. 8, pp. 116733–116743, 2020, doi: 10.1109/ACCESS.2020.3004611.

[44]   J. Lai, "Energy management strategy adopting power transfer device considering power quality improvement and regenerative braking energy utilization for double-modes traction system," *CPSS Transactions on Power Electronics and Applications*, vol. 7, no. 1, pp. 103–111, 2022, doi: 10.24295/cpsstpea.2022.00010.

[45]   R. R. Deshmukh, M. S. Ballal, and H. M. Suryawanshi, "A fuzzy logic based supervisory control for power management in multibus DC microgrid," *IEEE Transactions on Industry Applications*, vol. 56, no. 6, pp. 6174–6185, 2020, doi: 10.1109/TIA.2020.3012415.

BIOGRAPHIES OF AUTHORS

Adhi Kusmantoro 🆔 ⑧ SC ◖ is Assistant Professor in the Department of Electrical Engineering, Universitas PGRI Semarang, Indonesia. He holds a Ph.D. in Electrical Engineering with a specialization in power systems from Institut Teknologi Sepuluh Nopember (ITS) Surabaya, Indonesia in 2021. Master's degree in Electrical Engineering from Universitas Gadjah Mada (UGM), Yogyakarta, Indonesia in 2004. Bachelor's degree in Electrical Engineering Electrical Engineering from Universitas Semarang (USM), Semarang, Indonesia in 1999. His research areas are microgrids, smartgrids, power electronics, renewable energy, energy conversion and control systems. He is the head of the Electrical Engineering Department. He can be contacted at email: adhikusmantoro@upgris.ac.id.

Irna Farikhah 🆔 ⑧ SC ◖ is Assistant Professor at the department of Mechanical Engineering, Universitas PGRI Semarang, Indonesia. She holds a Ph.D. from Tokyo University of Agriculture and Technology, Japan. Master degree from Universitas Gadjah Mada (UGM), Yogyakarta, Indonesia. Bachelor degree from IKIP PGRI Semarang, Indonesia. The winner of the best student of IKIP PGRI Semarang, 2007. Finalist of the best Indonesian Student, 2007. A scholarship awardee from Indonesian government, 2017. A scholarship awardee from Turkish government, 2019. Her research areas are Efficiency of thermoacoustic engine and cooler/energy conversion and efficiency. She can be contacted at email: irnafarikhah@upgris.ac.id.